

Negative index of refraction observed in a single layer of closed ring magnetic dipole resonators

Zhao Hao^{a)} and Michael C. Martin^{b)}

Advanced Light Source Division, Lawrence Berkeley National Laboratory, 1 Cyclotron Rd, Berkeley, California 94720, USA

Bruce Harteneck and Stefano Cabrini

Molecular Foundry, Lawrence Berkeley National Laboratory, 1 Cyclotron Rd, Berkeley, California 94720, USA

Erik H. Anderson

Center for X-Ray Optics, Lawrence Berkeley National Laboratory, 1 Cyclotron Rd, Berkeley, California 94720, USA

(Received 14 August 2007; accepted 28 November 2007; published online 20 December 2007)

We report the results of a spectroscopic study of a single layer of metallic single closed ring resonators on freestanding thin membrane at near normal and grazing angles of incidence. When the magnetic component of the light is perpendicular to the ring plane, we observe a negative index of refraction down to -1 around 150 THz, attributed to a strong magnetic dipolar resonance and a broad electric resonance in this metamaterial. We experimentally identify the different resonance modes and the spectral region of negative refractive index on a series of samples with different feature and lattice sizes, comparing to electromagnetic simulations. © 2007 American Institute of Physics. [DOI: 10.1063/1.2825468]

Interest in artificially structured metamaterials has grown due to their ability to nonconventional interactions with light.^{1–4} One property which has attracted much attention is refraction with a negative index. Some exciting applications have been proposed and/or demonstrated primarily at gigahertz frequencies, including recently a “cloaking” device.⁵ Conducting split ring resonators have been widely used because the incident time-varying magnetic field of the light induces circulating currents and capacitance, similar to an inductor-capacitor (*LC*) circuit. Other authors⁶ have shown the existence of an electric coupling to these magnetic resonances⁷ at mid-or near-infrared frequencies. For example, two electric dipoles (or a quadrupole) can show a resonant response in an asymmetric structure with a frequency near the inherent magnetic resonance frequency.

This work has provided many insights, but it is becoming increasingly clear that realizing direct magnetic resonators at optical frequencies presents challenges. Resonators based on an *LC* oscillator require a linear ultrafast response to the field by the charge/current. The response of metals becomes nonlinear at frequencies beyond the terahertz range, so *LC* resonances couple too weakly for negative refraction. Recently, Sarychev *et al.*⁸ proposed an alternative called “magnetic plasmonic resonance.” Optical magnetic resonances can be excited in nanometer sized metallic structures through the excitation of plasmon oscillations, instead of geometric *LC* resonances. Plasmonics in nanometer sized metal structures is an interesting topic in itself as it may merge photonics and electronics for many novel applications.⁹

Plasmonic considerations may lead to another solution as we are demonstrating in this letter—constructing plasmonic magnetic dipole resonators to couple directly with the

magnetic component of light. Instead of using a gapped metal ring structure, we have constructed a metamaterial of magnetic dipoles using closed metal rings. Although other applications of plasmonic ring resonators have been discussed in recent years,¹⁰ we believe that their experimental use as high-frequency metamaterials is an exciting development.

We also show in this letter how to measure direct magnetic resonances by using a grazing angle (GA) incidence objective on a Fourier transform infrared (FTIR) microscope and how a multioscillator fit can be used to extract optical constants. By performing GA measurements and comparing to near-normal incidence measurements, we can identify resonances with different symmetry origins, specifically symmetric electric dipolar resonances and antisymmetric magnetic dipolar resonances in these closed ring structures. Because of the similarity between magnetic dipolar resonances and multipole electric resonances in composite metamaterials (for example, an electrically induced magnetic resonance⁷), we believe that this capability provides a convenient way to unravel the complex optical response of nanoscale resonators.

All FTIR spectroscopy measurements were performed using Thermo Fischer FTIR microscopes (Nic-Plan and Continuum XL) with a dry nitrogen purge. We used a thermal IR source or for higher spatial resolution the synchrotron source of the advanced light source beamline 1.4.3 or 1.4.4. KBr and CaF₂ beamsplitters were used to measure spectra ranging from 600 to 12000 cm⁻¹ (~18 to 360 THz). We used a standard Nicolet 15× all-reflective Cassegrain objective for near-normal incidence reflection and transmission measurements (~26° incidence angle), and a Bruker Optics GA incidence objective to measure reflection at ~83° incidence. When polarized appropriately, the GA objective creates a transverse electromagnetic wave on the surface of the sample.

^{a)}Electronic mail: zhao@lbl.gov.

^{b)}Electronic mail: mcmartin@lbl.gov.

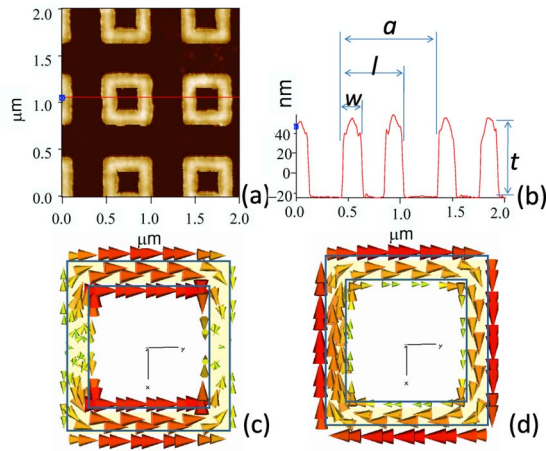


FIG. 1. (Color online) (a) AFM image of a closed ring nanoresonator sample. (b) Cross-section profile data measured along the straight line in (a). The linewidth $w \approx 100$ nm, the unit ring size $l \approx 500$ nm, the lattice constant $a \approx 900$ nm, and the thickness $t \approx 73$ nm, on a ~ 100 nm thick freestanding SiN_x membrane. (c) and (d) are simulated surface current distributions of an electric dipolar mode (E1) at ~ 4400 cm^{-1} and a magnetic dipolar mode (M1) at ~ 6000 cm^{-1} , respectively.

The metamaterial samples were made using electron beam lithography and gold plating on a 100 nm SiN_x substrate to make the metamaterials almost freestanding. A thin gold film is first deposited under the photoresist to provide a plating base electrode. The desired sample patterns are written into the photoresist which is developed exposing the plating base. Gold is plated to the desired thickness, the remaining photoresist is chemically removed, and finally the metallic plating base around the structures (and a small amount of the sample thickness) is etched off by plasma sputtering. This process yields structures with very sharp and straight edges, as shown in Fig. 1(a). The linewidth of the main sample discussed here is 100 nm and its thickness is ~ 78 nm as measured with an atomic force microscope (AFM), as shown in Fig. 1(b).

This closed ring structure can be conveniently simulated by commercially available EM simulation software (we use CST Microwave Studio) using the finite-difference time-domain (FDTD) method.¹¹ The simulated current distribution for two modes of interest is shown in Figs. 1(c) and 1(d), assuming perfect electric conductors. These are an electric dipole mode (E1) and a magnetic dipole mode (M1), having resonance frequencies of ~ 4400 and ~ 6000 cm^{-1} , respectively. The first order resonance frequency of an individual magnetic dipole can be determined by simply using¹²

$$f_r = \frac{2.405}{\sqrt{\mu\epsilon}L} = \frac{2.405c}{n_{\text{eff}}L}, \quad (1)$$

where L is the perimeter of the ring, c is the speed of light, and n_{eff} is the effective index of refraction determined by the surrounding material of the resonator. Therefore, the magnetic resonance frequency is inversely proportional to the ring size.

The lattice periodicity of the sample will affect the frequency, shape, and intensity of the resonances by changing the inter-ring coupling. We find that resonances, especially strong electric E1 resonances, become broader as the lattice constant decreases. By tuning the lattice constant, one can

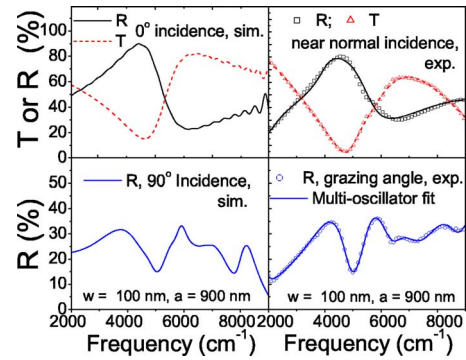


FIG. 2. (Color online) Transmission and reflection spectra of the metamaterial in Fig. 1. Results from FDTD simulations are on the left, while the data points in the right panels are experimental results. The solid or dashed curves on the right are multioscillator fits to the data.

get E1 and M1 to overlap over some frequency range, and thus create the conditions for negative refractive index.¹³

A nanofabricated sample with a 900 nm lattice constant and a 100 nm linewidth is simulated (on the left) and experimentally measured (on the right) in Fig. 2. We also fit the experimental data using a multioscillator model¹⁴ (solid and dashed lined on the right). In the near-normal incidence reflection and transmission measurements, we can clearly see a dominant electric resonance reflection peak at the frequency predicted by the FDTD simulation, corresponding to the E1 mode. In the GA reflection measurement with magnetic component of light perpendicular to the sample surface, a strong dip at ~ 5000 cm^{-1} is clearly visible corresponding to the overlapping E1 and M1 resonances.

In normal incidence, the symmetric E1 dominates, while in GA incidence, the antisymmetric M1 appears. Therefore, the difference between the normal and grazing incidence results is attributed to magnetic resonance(s). A group theoretical description of this type of planar resonator has been developed elsewhere.¹⁵

We rule out that the E1 and M1 modes are due to the periodicity of the structure by studying a series of samples having different lattice constants and different sizes. In both experiments and simulations, the resonance frequencies of both E1 and M1 scale only with the unit size of the resonator, not with the lattice constant. This is consistent with E1 and M1 being primary resonances of the individual rings, and not the periodic metamaterial array we have put them in. We note that although the wavelengths of interest are only two to three times larger than the lattice constants ($a = 600 - 900$ nm), which means we are no longer in the traditional effective medium limit,¹⁶⁻¹⁸ we do not experimentally find evidence that the observed resonances are impacted by the lattice periodicity.

Although there are subtle differences between the simulations and the experimental results, one can see that all features are reproduced. In this simulation, we use a lossy metal model with the conductivity of bulk gold for the ring resonator, and we assume incidence angles of exactly 0° or 90° . The experimental near-normal reflection data show an extra small dip at ~ 5000 cm^{-1} . This can be associated with a small z -axis component due to the 26° incidence angle allows a small coupling to M1 observed at this frequency in the GA measurements.

These observations lead us to conclude that we are indeed observing electric and magnetic couplings. We use a

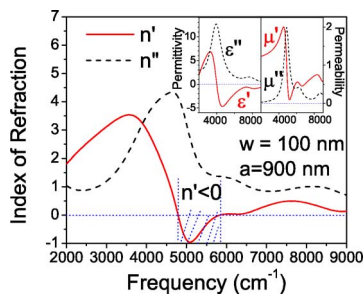


FIG. 3. (Color online) Real (n') and imaginary (n'') parts of the refractive index derived from the multioscillator fits to the experimental grazing angle reflection data shown in Fig. 2. The shaded spectral region indicates the region with negative refractive index. Real and imaginary parts of permittivity ϵ and permeability μ are shown in the inset.

multioscillator model to more accurately fit all the experimental features in Fig. 2. Simultaneously, we fit E1 in both normal incidence and GA incidence with a single strong electric oscillator at ~ 3800 cm^{-1} , and we fit M1, corresponding to the strong dip in GA measurement, by adding a pure magnetic oscillator at 4900 cm^{-1} . We found in the fit that the frequencies of both E1 and M1 oscillators are lower than what we obtained in the mode simulations using perfect electric conductors presumably due to considerable loss in gold thin films at such high frequencies. We convert the multioscillator fits into the real and imaginary parts of the index of refraction, as shown in Fig. 3. A significant spectral region (from 4800 to 5840 cm^{-1}) centered at 5093 cm^{-1} (153 THz) shows negative refractive index, down to $n' = -1.0$. The negative index is a result of the overlap of the E1 and M1 resonances, although a fully negative permeability is not achieved (minimum value of μ' is 0.09) due to the scattering loss¹⁹ (see inset of Fig. 3). However the strongly enhanced dip observed in the GA reflectivity is an indication of a large change in the refractive index, and therefore we believe that a so-called “double negative” material is also achievable with this type of resonator.

One can push the magnetic resonance frequency higher by reducing the circumference of the closed ring structures. We show data from a sample having a linewidth of 60 nm in Fig. 4. One can see that the resonance frequencies of E1 and M1 are now ~ 4500 and ~ 7000 cm^{-1} , respectively, although the dip is not as strong as the $w = 100$ nm sample. As shown in the inset of Fig. 4, there is a pronounced change in the resultant index of refraction, but it does not yet cross below zero. A finer tuning of the dimensions and lattice spacing is, however, needed to better couple the magnetic resonance and

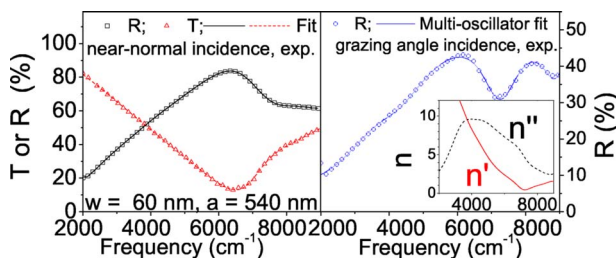


FIG. 4. (Color online) Transmission and reflection spectra of closed ring resonators with $w = 60$ nm and $a = 540$ nm. The data points are experimental measurements and the solid curves are multioscillator fits to the data. Inset: real and imaginary parts of the refractive index derived from the fit to the grazing angle reflection data.

the electric resonance in order to achieve a fully negative index of refraction. We also anticipate that the thickness of the SiN_x substrate, 100 nm, may introduce a significant loss at these frequencies. At higher frequencies, the metallic nanowires may also have increasing surface impedance and therefore increased loss. These issues may be mitigated by using an even thinner membrane substrate and materials with improved optical properties (for example, silver structures on 20 – 60 nm thick SiN_x membrane).

In summary, we have fabricated nanoscale metamaterials composed of individual closed ring magnetic dipole resonators. The experimentally observed resonance frequencies of 60 and 100 nm linewidth resonators are ~ 7000 cm^{-1} (~ 210 THz) and ~ 5000 cm^{-1} (~ 150 THz), respectively, well in the near-IR range. We show that negative index of refraction is obtained for the 100 nm resonators at ~ 5000 cm^{-1} (~ 150 THz). This experiment on magnetic dipolar resonators confirms the existence of magnetic dipolar moments in nanoparticles,^{20–22} and we continue to push negative refraction to even higher optical frequencies.

We gratefully acknowledge collaborations on the simulation software with John Byrd and Gang Huang of LBNL, and useful discussions with Willie J. Padilla and Nathan Landy of Boston College. This work was supported by the Laboratory Directed Research and Development Program and at Molecular Foundry by the Office of Science, Office of Basic Energy Sciences, of Lawrence Berkeley National Laboratory under the Department of Energy Contract No. DE-AC02-05CH11231.

¹V. G. Veselago, Sov. Phys. Usp. **10**, 509 (1968).

²D. R. Smith, Willie J. Padilla, D. C. Vier, S. C. Nemat-Nasser, and S. Schultz, Phys. Rev. Lett. **84**, 4184 (2000).

³R. A. Shelby, D. R. Smith, and S. Schultz, Science **299**, 77 (2001).

⁴J. B. Pendry, Phys. Rev. Lett. **85**, 3966 (2000).

⁵D. Schurig, J. J. Mock, B. J. Justice, S. A. Cummer, J. B. Pendry, A. F. Starr, and D. R. Smith, Science **314**, 977 (2006).

⁶S. Linden, C. Enkrich, M. Wegener, J. Zhou, T. Koschny, and C. M. Soukoulis, Science **306**, 1351 (2004).

⁷N. Katsarakis, T. Koschny, M. Kafesaki, E. N. Economou, and C. M. Soukoulis, Appl. Phys. Lett. **84**, 2943 (2004).

⁸A. K. Sarychev, G. Shvets, and V. M. Shalae, Phys. Rev. E **73**, 036609 (2006).

⁹E. Ozbay, Science **311**, 189 (2006).

¹⁰For example, X. Wang and K. Kempa, Phys. Rev. B **71**, 233101 (2005); B. Wang and G. P. Wang, Appl. Phys. Lett. **89**, 133106 (2006); T. Kipp, H. Welsch, Ch. Strelow, Ch. Heyn, and D. Heitmann, Phys. Rev. Lett. **96**, 077403 (2006).

¹¹D. Schurig, Int. J. Numer. Model. **19**, 215 (2006).

¹²J. D. Jackson, *Classical Electrodynamics*, 3rd Ed. (Wiley, New York, 1998).

¹³Z. Hao, M. C. Martin, B. Harteneck, S. Cabrini, E. H. Anderson, W. J. Padilla, APS Meeting, Denver, CO, March 2007 (unpublished).

¹⁴The fitting program was developed by Alexey Kuzmenko, University of Geneva (<http://optics.unige.ch/alexey/refit.html>).

¹⁵W. J. Padilla, Opt. Express **15**, 1639 (2007).

¹⁶R. Liu, T. J. Cui, D. Huang, B. Zhao, and D. R. Smith, Phys. Rev. E **76**, 026606 (2007).

¹⁷T. Driscoll, D. N. Basov, W. J. Padilla, J. J. Mock, and D. R. Smith, Phys. Rev. B **75**, 115114 (2007).

¹⁸T. Driscoll, G. O. Andreev, D. N. Basov, S. Palit, T. Ren, J. Mock, S.-Y. Cho, N. M. Jokerst, and D. R. Smith, Appl. Phys. Lett. **90**, 092508 (2007).

¹⁹S. Zhang, W. Fan, N. C. Panoiu, K. J. Malloy, R. M. Osgood, and S. R. J. Brueck, Phys. Rev. Lett. **95**, 137404 (2005).

²⁰E. Geneux and B. Wanders-Vincenz, Phys. Rev. Lett. **3**, 422 (1959).

²¹N. E. Russell, J. C. Garland, and D. B. Tanner, Phys. Rev. B **23**, 632 (1981).

²²A. Alù, A. Salandrino, and N. Engheta, Opt. Express **14**, 1557 (2006).